# Multifrequency Acoustooptic Diffraction

DAVID L. HECHT, MEMBER, IEEE

*Abstract*—A coupled mode formulation is developed for the analysis of acoustooptic diffraction with multiple acoustic waves at different carrier frequencies. For the Raman-Nath (thin ultrasonic grating) regime, analytic solutions are obtained for $N$ signals. In the Bragg (thick ultrasonic grating) limit, analytic solutions are obtained for two independent signals. Truncated series approximations for $N$ small signals are given for both regimes. The theory is applied to the quantitative evaluation of linear and nonlinear effects occurring in acoustooptic spectrum analysis, optical information processing, multichannel recording, and multiple beam deflection and modulation. These include diffraction efficiency, compression, cross modulation, and spurious intermodulation intensities. The results show that all nonlinear effects considered are substantially reduced in the Bragg limit. This is supported by experimental measurements of the various effects, in good agreement with the Bragg limit theory.

## I. Introduction

DIFFRACTION of a light beam by multiple simultaneous acoustic waves occurs in a number of acoustooptic applications including radio frequency spectrum analysis [1]-[3], real-time signal processing [4]-[8], multichannel recording [2], [9], multiple beam deflection and modulation [10], and frequency coded television display [5]. When multiple finite amplitude acoustic waves diffract a laser beam, multiple diffracted beams are generated, and a number of nonlinear effects occur [11]. These include cross modulation in the amplitudes of the diffracted beams and the generation of additional (spurious) intermodulation beams [1], [11]. These effects establish intrinsic limits for the dynamic range [1], [3], [7] and maximum diffraction efficiencies [10] in multifrequency acoustooptic applications.

The diffraction of a plane wave monochromatic light beam by a single sound beam has been reviewed and analyzed by W. R. Klein and D. B. Cook [12], [13] using a coupled mode formulation. By generalizing this formulation to include multiple acoustic waves of different carrier frequencies, multifrequency diffraction effects can be quantitatively analyzed. These include diffraction efficiencies, cross modulation, and intermodulation mode amplitudes. The physical assumptions and mathematical notation are compatible with the analyses of Klein and Cook [12], [13], except for the generalization to multiple signals. In particular, it is assumed that the modulation of the index of refraction due to a sinusoidal input is purely sinusoidal. Then all nonlinear optical responses are due to multiple linear acoustooptic diffraction processes rather than photoelastic or acoustic nonlinearities [14]. The results give lower bounds for acoustooptic diffraction nonlinearities, independent of material nonlinearities. These are compared with experimental results for a glass acoustooptic deflector.

Manuscript received February 25, 1976.

The author is with the Applied Technology Division, Itek Corporation, Sunnyvale, CA 94086.

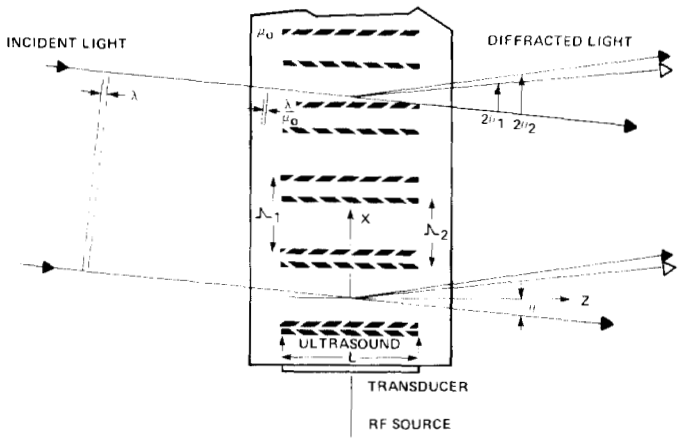


Fig. 1. Multifrequency acoustooptic diffraction geometry.

The interaction geometry is shown in Fig. 1. The sound waves of frequencies $f_1$ and $f_2$ with corresponding acoustic wavelengths $\Lambda_1$ and $\Lambda_2$ are illustrated propagating with velocity $V_s$ along the $X$ direction in an optically isotropic medium with index of refraction $\mu_0$. The thickness of the ultrasonic gratings along the $Z$ axis is $L$. A collimated beam of light of freespace wavelength $\lambda$ is incident on the sound field at an angle $\theta$ from the $Z$ axis, in the $XZ$ plane.

Each sound wave interacting with the light beam will generate a principal diffracted beam separated from the incident beam by an angle (measured in the medium) $2\theta_i$:

$$2\theta_i = 2\sin^{-1}\left(\frac{\lambda f_i}{2\mu_0 V_s}\right) \approx \left(\frac{\lambda}{\mu_0 V_s}\right) f_i, \quad \theta_i < 0.1 \text{ rad.}$$

This frequency dispersion of the acoustooptic grating is the basis for the use of acoustooptic devices in optical deflection, spectrum analysis at radio and microwave frequencies, and multibeam recording. However, the generation of various diffracted beams is not completely independent. Each generated beam depletes the source beam from which all the principal beams are generated. In addition, light in each principal beam may be rediffracted by another acoustooptic grating. This produces cross modulation and generates intermodulation beams corresponding to sum and difference frequencies $f_i \pm f_j$. In turn, additional intermodulation beams may be generated. Fig. 2 illustrates the dominant beams which may be generated when two signals are present. Labeling of the modes corresponds to the frequency shift from the source beam frequency using radio frequency analysis nomenclature. The corresponding frequency shifts are indicated. The angular deflection of each beam from the source beam is proportional to the fre-

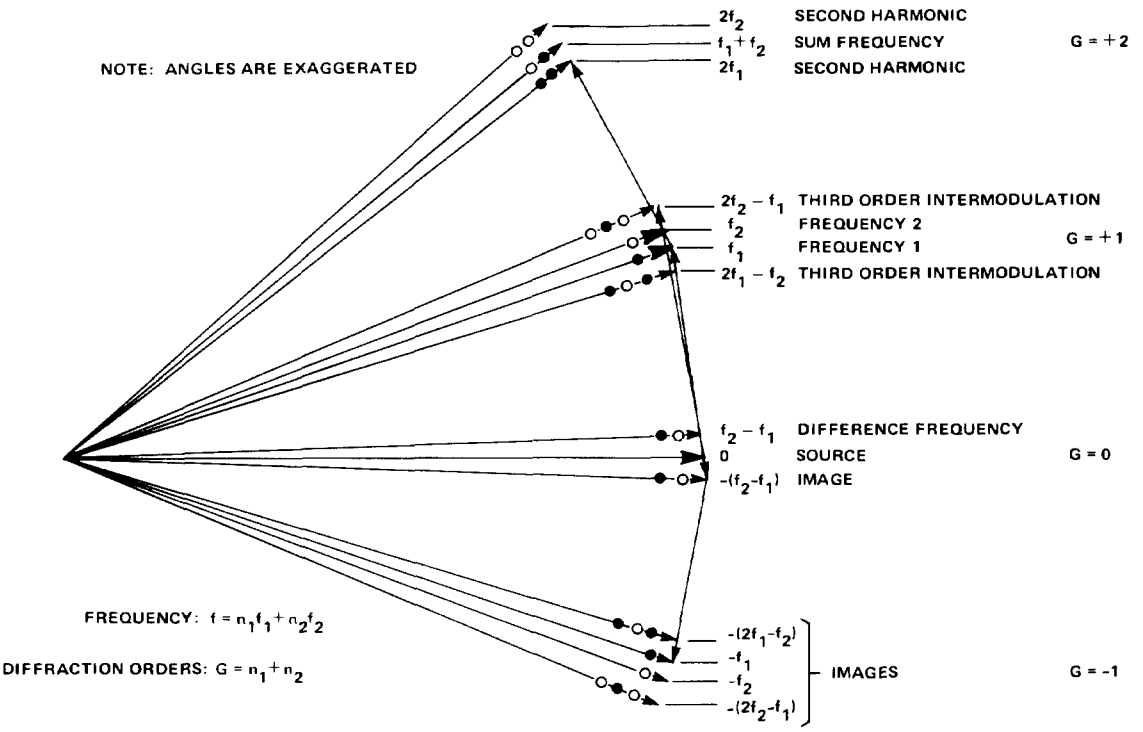


Fig. 2. Acoustooptic generation of intermodulation modes.

quency shift. As in single frequency diffraction, the beams divide naturally into diffraction orders: $G = 0, \pm1, \pm2, \cdots$. The strongest intermodulation modes which interfere spatially with the principal modes in the first diffraction order correspond to frequencies $2f_i - f_j$ and are conventionally termed third-order[1] intermodulation products because they result from a third-order interaction. This effect limits spurious free dynamic range. A typical intensity spectrum is shown in Fig. 3.

The objective of this work is to investigate quantitatively and qualitatively various multifrequency diffraction effects, comparing thick (Bragg) and thin (Raman-Nath) acoustooptic diffraction devices.

## II. Theory

The optical wave equation for the electric intensity is

$$\nabla^2 E = \frac{[\mu(x,t)]^2}{c^2}\frac{\partial^2 E}{\partial t^2} \tag{1}$$

where the refractive index in the region of the sound field $(0 < z < L)$ may be written as

$$\mu(x,t) = \mu_0 + \sum_{m=1}^{N} \mu_m \sin\left[(\omega_m^* t - k_m^* x) + \delta_m\right] \tag{2}$$

where $\omega_m^*$ and $k_m^*$ are the circular frequency and wavenumber of the acoustic signal of wavelength $\Lambda_m$; $\mu_m$ and $\delta_m$ are the amplitude and phase of the refractive index modulation due to the $m$th signal. $\mu_0$ is the unperturbed index of refraction,

[1]To avoid confusion between diffraction order and interaction order, the word order used alone will be used to refer to interaction order.

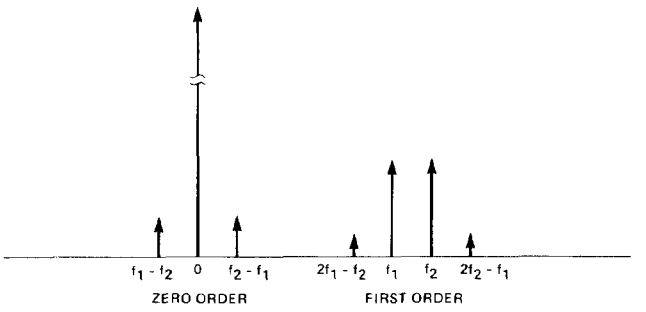


Fig. 3. Two-tone intermodulation spectrum.

assumed constant for all modes (i.e., excluding birefringent diffraction [15]). A total of $N$ signals is considered.

The general Fourier series for the electric intensity is an $N$-tuple expansion:

$$E = \exp(i\omega t) \sum_{n_1=-\infty}^{\infty} \sum_{n_2=-\infty}^{\infty} \cdots \sum_{n_N=-\infty}^{\infty} \Psi_{(\bar{n})} \cdot \exp\left[i \sum_{m=1}^{N} n_m(\omega_m t + \delta_m) - i\vec{k}_{(\bar{n})} \cdot \vec{r}\right] \tag{3}$$

where

$$\vec{k}_{(\bar{n})} \cdot \vec{r} = \mu_0 k(z\cos\theta + x\sin\theta) + \sum_{m=1}^{N} n_m k_m^* x \tag{4}$$

$(\bar{n})$ represents $(n_1, n_2, \cdots, n_N)$ and $\omega$ and $k$ are the circular frequency and wavenumber for the light. $n_m$ may take any positive or negative integer values.

Equation (3) indicates that the circular frequency for mode $\Psi_{(\bar{n})}$ is

$$\omega + \sum_{m=1}^{N} n_m \omega_m^*$$

so that all intermodulation modes are represented as well as the harmonic diffraction modes present in the single frequency case [12]. Each diffraction order contains an infinite multiplicity of modes, corresponding to all combinations of values for the various $n_m$ such that $\Sigma n_m = G_{(\bar{n})}$, the number of the order.

*Coupled Mode Equations*

By substituting (2)-(4) into the optical wave equation, assuming small variation in $\Psi_{(\bar{n})}$ over optical wavelength distances and optical cycle time periods, and neglecting quadratic terms in $|\mu_m|$, an infinite set of coupled mode equations is obtained:

$$\frac{d}{dz}\Psi_{(\bar{n})} - i\left[\frac{\left(\sum_{m=1}^{N} n_m k_m^*\right)^2}{2\mu_0 k\cos\theta} + \tan\theta \sum_{m=1}^{N} n_m k_m^*\right]\Psi_{(\bar{n})} = \sum_{m=1}^{N} \frac{k\mu_m}{2\cos\theta}\left[\Psi_{(\bar{n}+\bar{a}_m)} - \Psi_{(\bar{n}-\bar{a}_m)}\right] \tag{5}$$

where

$(\bar{n})$ represents $(n_1, n_2, \cdots, n_{N-1}, n_N)$,

$(\bar{n} - \bar{a}_m)$ represents $(n_1, n_2, \cdots, n_{m-1}, n_m - 1, n_{m+1}, \cdots, n_{N-1}, n_N)$,

$(\bar{n} + \bar{a}_m)$ represents $(n_1, n_2, \cdots, n_{m-1}, n_m + 1, n_{m+1}, \cdots, n_{N-1}, n_N)$.

Equation (5) is the multiple signal generalization of the acoustooptic coupled mode equations [12], [13]. At this point normalized parameters [12] may be introduced to simplify the analysis of parameters:

$$V_m \doteq k\mu_m L/\cos\theta \tag{6}$$

$$Q \doteq \frac{\bar{k}^{*2} L}{\mu_0 k\cos\theta} \tag{7}$$

$$\alpha \doteq (\mu_0 k/\bar{k}^*)\sin\theta \tag{8}$$

$$G_{(\bar{n})} \doteq \sum_{m=1}^{N} n_m \tag{9}$$

$$\beta_m \doteq (k_m^* - \bar{k}^*)/\bar{k}^* \tag{10}$$

and $n_1, n_2, \cdots, n_N$ take all integer values. $V_m$ is the normalized index of refraction modulation amplitude corresponding to $\mu_m$. $\alpha$ is a measure of the angle of incidence of the light on the sound field, normalized to the angle between diffraction orders. $Q$ is a measure of the angle between diffraction orders, normalized to the diffraction spread angle of the sound field. These parameters correspond to those in the single frequency analysis [12], [13], except that the $V_m$ terms allow for multiple signals and $\alpha$ and $Q$ are defined with respect to the midband wavenumber $\bar{k}^*$. In addition, $\beta_m$ is the fractional deviation of the signal wavenumber $k_m^*$ from $\bar{k}^*$, and $G_{(\bar{n})}$ is the diffraction order index, defined previously.

Some important examples of values for the normalized parameters are $Q \ll 1$ in the Raman-Nath diffraction regime; $Q > 4\pi$ in the Bragg diffraction regime; $\alpha = 0$ at normal incidence, $|\alpha| = \frac{1}{2}$ for Bragg incidence at midband; and $|\beta_m| < \frac{1}{3}$ for frequencies within an octave band.

An additional useful parameter is the interaction order index:

$$D_{(\bar{n})} = \sum_{m=1}^{N} |n_m|. \tag{11}$$

$D$ is the minimum number of coupling interactions involved in the generation of a particular mode. $D$ determines the small signal power dependence of the intensity of the mode.

Using the normalized parameters, the coupled mode equations take the form:

$$\frac{d}{dz}\Psi_{(\bar{n})} - i\Delta K_{(\bar{n})}\Psi_{(\bar{n})} + \sum_{m=1}^{N} \frac{V_m}{2L}\left[\Psi_{(\bar{n}-\bar{a}_m)} - \Psi_{(\bar{n}+\bar{a}_m)}\right] = 0 \tag{12}$$

where

$$\Delta K_{(\bar{n})} = \frac{Q}{2L}\left(G_{(\bar{n})} + \sum_{m=1}^{N} n_m\beta_m\right)\left(G_{(\bar{n})} - 2\alpha + \sum_{m=1}^{N} n_m\beta_m\right). \tag{13}$$

$\Delta K_{(\bar{n})}$ is the wavevector mismatch or phase mismatch per unit interaction length of mode $\Psi_{(\bar{n})}$ relative to the source mode $\Psi_{(\bar{0})}$, for which $n_m \equiv 0$.

Although the coupled mode set for the multifrequency problem is more elaborate than the single frequency analysis, important characteristics are maintained. Modes whose orders $G_{(\bar{n})}$ differ by one and whose frequencies differ by $\omega_m$ are coupled by the term $V_m$.

*Phase Match Condition*

When the accumulated phase mismatch over the interaction length $\Delta KL$ is below $\pi/2$ radians, unidirectional power flow between the modes occurs. For larger mismatch the power flow is oscillatory over the path $L$, and cumulative energy transfer is limited.

*Initial Conditions*

The initial conditions for the diffraction problem place all energy in the source mode at $z = 0$:

$$\Psi_{(\bar{0})} = 1 \tag{14a}$$

$$\Psi_{(\bar{n})} = 0, \quad \text{otherwise.} \tag{14b}$$

*Coupled Mode Equation Solutions*

Explicit literal solutions to the coupled mode equations can be found only under limited conditions. The solutions pre-

sented here have been found most useful in investigation of the qualitative and quantitative behavior of multifrequency acoustooptic diffraction effects.

*Raman-Nath Regime ($Q \ll 1$)*

The infinite coupled mode set for all modes can be solved analytically in the Raman-Nath regime subject to the approximation:

$$\frac{Q}{2} \sum_{m=1}^{N} n_m (1 + \beta_m) < \frac{\pi}{2} \tag{15}$$

so that

$$\Delta K \approx -\frac{Q\alpha}{L} \sum_{m=1}^{N} n_m (1 + \beta_m). \tag{16}$$

This type of approximation [16] underestimates the wavevector mismatch for high-order modes ($D > 3$), and hence leads to overestimation of the amplitudes for these modes. However, these modes typically have very small amplitudes and do not appreciably affect the amplitudes of the principal modes, which are of primary interest.

The differential equations in this case become

$$\frac{d}{dz} \Psi_{(\bar{n})} + \sum_{m=1}^{N} \frac{V_m}{2L} \left[ \Psi_{(\bar{n}-\bar{a}_m)} - \Psi_{(\bar{n}+\bar{a}_m)} \right] + \frac{in_m Q\alpha(1 + \beta_m)}{L} \Psi_{(\bar{n})} = 0. \tag{17}$$

Solution to (17) can be obtained in the product form:

$$\Psi_{(\bar{n})} = \prod_{m=1}^{N} \phi_{n_m}(V_m) \tag{18}$$

which converts (17) to the form:

$$\sum_{m=1}^{N} \left( \frac{\Psi_{(\bar{n})}}{\phi_{n_m}} \right) \left[ \frac{d}{dz} \phi_{n_m} + \frac{V_m}{2L} \left( \phi_{(n_m - 1)} - \phi_{(n_m + 1)} \right) + \frac{in_m Q\alpha(1 + \beta_m)}{L} \phi_{n_m} \right] = 0. \tag{19}$$

Equation (19) is a sum of expressions nearly identical to the corresponding single frequency differential equation in the Raman-Nath regime [12]. The equation is satisfied if each expression is equal to zero. This is true provided:

$$\phi_{n_m} = \exp \left[ -in \frac{Q\alpha(1 + \beta_m) z}{2L} \right] |\phi_{n_m}| (-1)^n \tag{20a}$$

$$|\phi_{n_m}| = J_{n_m} \left[ \frac{2V_m}{Q\alpha(1 + \beta_m)} \sin \left( \frac{Q\alpha(1 + \beta_m) V_m z}{2L} \right) \right] \tag{20b}$$

where $J_{n_m}$ is the Bessel function of integer order $n_m$ with argument given in brackets.

Each $\phi_{n_m}$ is identical to a single frequency Raman-Nath diffraction solution for the $n_m$ diffraction order due to signal amplitude $V_m$ when the (normalized) angle of incidence is $\alpha(1 + \beta_m)$. Mode amplitudes at the end of the interaction are obtained with $z = L$.

*Bragg Regime ($Q > 4\pi$)*

In the Bragg regime, wavevector mismatch can only be minimized for one diffraction order besides zeroth order, as established by the value of $\alpha$. In most practical applications, $\alpha \approx \pm\frac{1}{2}$, matching order $G = \pm 1$. Similar results are obtained in either case.

With Bragg incidence at midband in the positive first order, $\alpha = +\frac{1}{2}$, the wavevector mismatch is given as follows. For modes in the zeroth order, $G = 0$,

$$\Delta KL \approx -\frac{Q}{2} \sum_{m=1}^{N} n_m \beta_m. \tag{21}$$

For modes in the first order, $G = 1$,

$$\Delta KL \approx \frac{Q}{2} \sum_{m=1}^{N} n_m \beta_m. \tag{22}$$

For modes in other orders,

$$\Delta KL \approx \frac{Q}{2} (G)(G - 1). \tag{23}$$

The approximate forms, (21)-(23) apply provided:

$$\sum_{m=1}^{N} n_m \beta_m \ll 1. \tag{24}$$

This holds for moderate fractional bandwidth $\beta_i \ll 1$, except for high-order modes ($D \gg 1$), which typically have very small amplitudes. As a result, wavevector mismatch may be considered small for modes in the zeroth and first order:

$$|\Delta KL| < \frac{\pi}{2}. \tag{25}$$

However, wavevector mismatch in other orders is large:

$$|\Delta KL| \approx \frac{Q}{2} |(G)(G - 1)| > 4\pi \gg \frac{\pi}{2}. \tag{26}$$

In the following approximation, modes outside zero and first order are dropped, and wavevector mismatch within the zero and first orders is neglected. The coupled mode equations for orders zero and one reduce to two sets:

$$\frac{d}{dz} \Psi^0_{(\bar{n})} = \sum_{m=1}^{N} \frac{V_m}{2L} \Psi^1_{(\bar{n}+\bar{a}_m)} \tag{27a}$$

$$\frac{d}{dz} \Psi^1_{(\bar{n})} = -\sum_{m'=1}^{N} \frac{V_{m'}}{2L} \Psi^0_{(\bar{n}-\bar{a}_{m'})} \tag{27b}$$

where the superscripted $\Psi^G_{(\bar{n})}$ indicates the order of the mode.

One equation of the form (27a) or (27b) occurs for each mode in the zeroth order or first order, respectively. Complete analytic solution sets have been found for $N = 2$. The solutions for all modes $\Psi^0_{(\bar{n})}$ and $\Psi^1_{(\bar{n})}$ and arbitrary values for $V_1$ and $V_2$ are derived in Appendix A.

The solutions are in the form of power series

$$\Psi^0_{(n,-n)} = \sum_{r=0}^{\infty} a_{nr} z^r \tag{28}$$

$$\Psi^1_{(n,-n+1)} = \sum_{r=0}^{\infty} \left(\frac{-1}{r+1}\right) \left[\frac{V_1}{2L} a_{(n-1)r} + \frac{V_2}{2L} a_{nr}\right] z^{r+1} \tag{29}$$

where

$$a_{nr} = \sum_{s=0}^{[(M-|n|)/2]} C_{M,n,s} \frac{(-1)^M}{(r)!} \left(\frac{V_1 V_2}{4L^2}\right)^{2s+|n|} \cdot \left(\frac{V_1^2 + V_2^2}{4L^2}\right)^{M-|n|-2s} \tag{30}$$

$[x]$ denotes greatest integer [17] not greater than $x$

$$M \doteq \frac{r}{2} \tag{31}$$

$$C_{M,n,s} \doteq \left(\frac{M!}{(M - |n| - 2s)!\,(s + |n|)!\,s!}\right). \tag{32}$$

Mode amplitudes at the end of the interaction are obtained with $z = L$.

$C_{M,n,s}$ is the number of pathways for diffraction from mode $\Psi^0_{(0)}$ to mode $\Psi^0_{(n)}$ in $M$ pairs of interactions including: $(M - |n| - 2s)$ up-conversions from $G = 0$ to $G = 1$ followed with down-conversion driven by the same frequency; $(s + |n|)$ up-conversions driven by $\omega_1^*$ followed with down-conversion driven by $\omega_2^*$; and $s$ up-conversions driven by $\omega_2^*$ followed with down-conversion at $\omega_1^*$. For negative $n$, the roles of $\omega_2^*$ in this description are interchanged. The total frequency shift is $n(\omega_1 - \omega_2)$ for any $n$.

Thus the number of phase-matched interaction pathways has a direct effect on the various mode amplitudes. The chief cause for the suppression of intermodulation and cross modulation effects in the Bragg regime compared to the Raman-Nath regime is the elimination of pathways branching outside orders 0 and 1.

For the special case $V_1 = V_2 = V$, it can be shown that the two-signal Bragg regime solutions are equal to ordinary Bessel functions of argument $V$ and order equal to the interaction order of the mode, i.e.,

$$\Psi^0_{n,-n} = (-1)^n J_{D_n}(V) \tag{33a}$$

$$\Psi^1_{n,-n+1} = (-1)^{n+1} J_{D_n}(V). \tag{33b}$$

This is an important reference case for intermodulation intensity.

Another special case of interest is zero amplitude for one signal, e.g., $V_2 = 0$. Then,

$$|\Psi^0_{0,0}| = \left|\cos\frac{V}{2}\right| \tag{34a}$$

$$|\Psi^1_{1,0}| = \left|\sin\frac{V}{2}\right| \tag{34b}$$

$$|\Psi_{n_1,n_2}| = 0, \quad \text{otherwise.} \tag{34c}$$

This checks with the well-known single signal solution [12] for exact Bragg incidence. The series solution method is applicable for an arbitrary number of signals $N$, and truncated series solutions for $N > 2$ are included in the following section.

## III. Interpretation and Results

Multifrequency diffraction effects may be quantitatively defined and related to the coupled mode amplitudes. For convenient reference, the results cited are summarized in Tables I–IV. Table I includes the analytic results for two independent signals, comparing the Raman-Nath regime at normal incidence with the Bragg regime at Bragg incidence. These are the most typical geometries. Table II gives the corresponding truncated series solutions which are applicable for small signals, $|V/2|^2 \ll 1$. Table III gives the generalization of the truncated series solutions to $N > 2$, which are derived from the analytic solution in the Raman-Nath regime and separately derived in the Bragg regime. Table IV gives the analytic solutions and small signal approximation for two equal amplitude signals. These provide the characteristic two-tone intermodulation spectrum.

TABLE I
Analytic Results—Two Signals

| | Symbol | Raman-Nath Regime $\alpha=0$ $Q\ll1$ | Bragg Regime* $\alpha=\pm\frac{1}{2}$ $Q>4\pi$ |
|---|---|---|---|
| Diffraction Efficiency | $I_{1,o}$ | $\lvert J_1(V_1)J_o(V_2)\rvert^2$ | $\lvert\Psi^1_{1,o}\rvert^2$ |
| Depletion | d | $1 - \lvert J_o(V_1)J_o(V_2)\rvert^2$ | $1 - \lvert\Psi^o_{o,o}\rvert^2$ |
| Compression | $C_1$ | $1 - \lvert\frac{2}{V_1}J_1(V_1)J_o(V_2)\rvert^2$ | $1 - \lvert\frac{2}{V_1}\Psi^o_{o,o}\rvert^2$ |
| Cross Modulation | $M_{1,2}$ | $1 - \lvert J_o(V_2)\rvert^2$ | $1 - \left\lvert\frac{\Psi_{1,o}}{\sin\left(\frac{V_1}{2}\right)}\right\rvert^2$ |
| Intermodulation $(2f_1-f_2)$ (two-tone third order) | $I_{2,1}$ | $\lvert J_2(V_1)J_1(V_2)\rvert^2$ | $\lvert\Psi^1_{2,1}\rvert^2$ |
| Intermodulation $(f_1-f_2)$ (difference) | $I_{1,-1}$ | $\lvert J_1(V_1)\rvert^2\lvert J_1(V_2)\rvert^2$ | $\lvert\Psi^o_{1,-1}\rvert^2$ |

* $\Psi_{n_1,n_2}$ given by Equations (28) to (32)

TABLE II
SMALL SIGNAL RESULTS—TWO SIGNALS

| | Symbol | Raman-Nath Regime $\alpha = 0$ $Q \ll 1$ | Bragg Regime $\alpha = \pm\frac{1}{2}$ $Q > 4\pi$ |
|---|---|---|---|
| Diffraction Efficiency | $I_{1,}$ | $\left(\frac{V_1}{2}\right)^2\left[1-\left(\frac{V_1}{2}\right)^2-2\left(\frac{V_2}{2}\right)^2\right]$ | $\left(\frac{V_1}{2}\right)^2\left[1-\frac{1}{3}\left(\frac{V_1}{2}\right)^2-\frac{2}{3}\left(\frac{V_2}{2}\right)^2\right]$ |
| Depletion | d | $2\left[\left(\frac{V_1}{2}\right)^2+\left(\frac{V_2}{2}\right)^2\right]$ | $\left[\left(\frac{V_1}{2}\right)^2+\left(\frac{V_2}{2}\right)^2\right]$ |
| Compression | $C_1$ | $\left[\left(\frac{V_1}{2}\right)^2+2\left(\frac{V_2}{2}\right)^2\right]$ | $\frac{1}{3}\left[\left(\frac{V_1}{2}\right)^2+2\left(\frac{V_2}{2}\right)^2\right]$ |
| Cross Modulation | $M_{1,2}$ | $2\left(\frac{V_2}{2}\right)^2$ | $\frac{2}{3}\left(\frac{V_2}{2}\right)^2$ |
| Intermodulation (Two-Tone-Third Order) | $I_{2,1}$ | $\frac{1}{4}\left(\frac{V_1}{2}\right)^4\left(\frac{V_2}{2}\right)^2$ | $\frac{1}{36}\left(\frac{V_1}{2}\right)^4\left(\frac{V_2}{2}\right)^2$ |
| Intermodulation ($f_1$-$f_2$) (difference) | $I_{1,-1}$ | $\left(\frac{V_1}{2}\right)^2\left(\frac{V_2}{2}\right)^2$ | $\frac{1}{4}\left(\frac{V_1}{2}\right)^2\left(\frac{V_2}{2}\right)^2$ |
| Intermodulation ($f_1$+$f_2$) (sum) | $I_{1,1}$ | $\left(\frac{V_1}{2}\right)^2\left(\frac{V_2}{2}\right)^2$ | --- |

TABLE III
SMALL SIGNAL RESULT—$N$ SIGNALS

| Characteristic | Symbol | Raman-Nath Regime $\alpha = 0$ $Q \ll 1$ | Bragg Regime $\alpha = \pm\frac{1}{2}$ $Q > 4\pi$ |
|---|---|---|---|
| Diffraction Efficiency | $I_{1,0,0\ldots}$ | $\left\lvert\frac{V_1}{2}\right\rvert^2\left[1-\left\lvert\frac{V_1}{2}\right\rvert^2-2\sum_{\ell=2}^{N}\left\lvert\frac{V_\ell}{2}\right\rvert^2\right]$ | $\left\lvert\frac{V_1}{2}\right\rvert^2\left[1-\frac{1}{3}\left\lvert\frac{V_1}{2}\right\rvert^2-\frac{2}{3}\sum_{\ell=2}^{N}\left\lvert\frac{V_\ell}{2}\right\rvert^2\right]$ |
| Depletion | d | $2\sum_{\ell=1}^{N}\left\lvert\frac{V_\ell}{2}\right\rvert^2$ | $\sum_{\ell=1}^{N}\left\lvert\frac{V_\ell}{2}\right\rvert^2$ |
| Compression | $C_{1,0,0\ldots}$ | $\left(\frac{V_1}{2}\right)^2+2\sum_{\ell=2}^{N}\left(\frac{V_\ell}{2}\right)^2$ | $\frac{1}{3}\left[\left(\frac{V_1}{2}\right)^2+2\sum_{\ell=2}^{N}\left(\frac{V_\ell}{2}\right)^2\right]$ |
| Cross Modulation | $M_{1,2}$ | $2\left(\frac{V_2}{2}\right)^2$ | $\frac{2}{3}\left(\frac{V_2}{2}\right)^2$ |
| Intermodulation (Two-Tone Third Order) | $I_{2,-1,0,0\ldots}$ | $\frac{1}{4}\left(\frac{V_1}{2}\right)^4\left(\frac{V_2}{2}\right)^2$ | $\frac{1}{36}\left(\frac{V_1}{2}\right)^4\left(\frac{V_2}{2}\right)^2$ |
| Three-Tone Third Order | $I_{1,-1,1,0,0\ldots}$ | $\left(\frac{V_1}{2}\right)^2\left(\frac{V_2}{2}\right)^2\left(\frac{V_3}{2}\right)^2$ | $\frac{1}{9}\left(\frac{V_1}{2}\right)^2\left(\frac{V_2}{2}\right)^2\left(\frac{V_3}{2}\right)^2$ |
| Difference | $I_{1,-1}$ | $\left(\frac{V_1}{2}\right)^2\left(\frac{V_2}{2}\right)^2$ | $\frac{1}{4}\left(\frac{V_1}{2}\right)^2\left(\frac{V_2}{2}\right)^2$ |

*Diffraction Efficiency $I_i$*

The diffraction efficiency $I_i$ of signal $V_i$ is the intensity of the corresponding principal (first-order) mode in the first diffraction order

$$I_i \doteq |\Psi_{(\bar{a}_i)}|^2. \tag{35}$$

For small signals (Tables II and III) diffraction efficiencies are approximately equal to the normalized drive intensity $(V/2)^2$ in both the Raman-Nath and Bragg regimes, independent of the number of signals:

$$I_i \approx \left(\frac{V_i}{2}\right)^2, \quad V_i < 0.1 \tag{36}$$

However, the deviation from linear response is more severe in the Raman-Nath regime and increases with the number of signals. This deviation is characterized quantitatively as compression and cross modulation (see below).

TABLE IV
RESULTS FOR TWO EQUAL AMPLITUDE SIGNALS

| Characteristic | Symbol | Raman-Nath Regime $\alpha=0$ $Q\ll1$ | Bragg Regime $\alpha=\pm\frac{1}{2}$ $Q>4\pi$ |
|---|---|---|---|
| Diffraction Efficiency | $I_{1,0}$ | $\lvert J_1(V)J_0(V)\rvert^2 \simeq \lvert\frac{V}{2}\rvert^2\left[1-3\left(\frac{V}{2}\right)^2\right]$ | $\lvert J_1(V)\rvert^2 \simeq \lvert\frac{V}{2}\rvert^2\left[1-\left(\frac{V}{2}\right)^2\right]$ |
| Maximum Diffraction Efficiency | | 0.115 at $V = 1.10$ | 0.339 at $V = 1.841$ |
| Depletion | d | $1-\lvert J_0(V)\rvert^4 \simeq 4\left(\frac{V}{2}\right)^2$ | $1-\lvert J_0(V)\rvert^2 \simeq 2\left(\frac{V}{2}\right)^2$ |
| Compression | $C_{1,0}$ | $1-\lvert\frac{2}{V}J_1(V)J_0(V)\rvert^2 \simeq 3\left(\frac{V}{2}\right)^2$ | $1-\lvert\frac{2}{V}J_1(V)\rvert^2 \simeq \left(\frac{V}{2}\right)^2$ |
| Cross Modulation | $M_{1,2}$ | $1-\lvert J_0(V)\rvert^2 \simeq 2\left(\frac{V}{2}\right)^2$ | $1-\left\lvert\frac{J_1(V)}{\sin\left(\frac{V}{2}\right)}\right\rvert^2 \simeq \frac{2}{3}\left(\frac{V}{2}\right)^2$ |
| Intermodulation (Two-Tone Third Order) | $I_{2,-1}$ | $\lvert J_2(V)J_1(V)\rvert^2 \simeq \frac{1}{4}\left(\frac{V}{2}\right)^6$ | $\lvert J_3(V)\rvert^2 \simeq \frac{1}{36}\left(\frac{V}{2}\right)^6$ |
| Third Order Intercept | $I_{1,0} = I_{2,-1}$ | $\left(\frac{V}{2}\right)^2 = 2$ | $\left(\frac{V}{2}\right)^2 = 6$ |

Theoretical diffraction efficiencies for two equal signals are plotted in Fig. 4 as a function of drive intensity $(V/2)^2$ for the Bragg and Raman-Nath limits. The Bragg diffraction efficiency (Table I) is determined by the first-order ordinary Bessel function $J_1(V)$; thus it is identical to the Raman-Nath diffraction efficiency for one signal [12] with a peak value of 0.339 at $V = 1.84$. This compares with a peak value of 1 at $V = \pi$ for one signal in the Bragg regime. Two-tone Raman-Nath maximum diffraction efficiency is further lowered to a peak value of 0.115 at $V = 1.1$. Experimental data correspond to a Bragg regime glass deflector $Q \approx 30$.

*Depletion*

Depletion is the reduction in intensity of the source mode $|\Psi_{(\bar{0})}|^2$ due to the finite intensities of the various diffracted beams:

$$d \doteq 1 - |\Psi_{(\bar{0})}|^2. \tag{37}$$

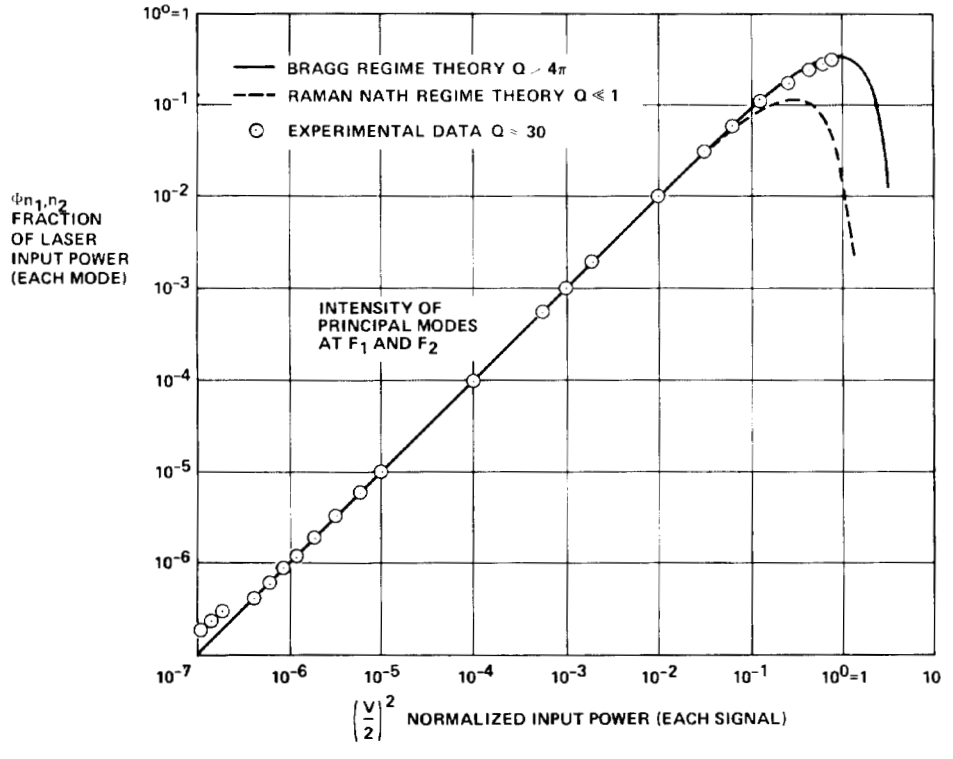


Fig. 4. Two-signal principal mode intensities ($V_1 = V_2 = V$).

Depletion is one source of the deviation from linear response in the principal first-order modes. In the small signal approximation, the depletion is equal to the total intensity in the principal first-order modes. For given signal amplitudes ($V_i$), depletion is twice as great in the Raman-Nath regime as in the Bragg regime because of the simultaneous generation of positive and negative first diffraction order modes. The various small signal results (Tables II and III) can be used, provided that the depletion of the source mode is less than 50 percent.

*Compression $C_i$*

Compression is defined as the total fractional deviation from linear response in the diffraction efficiency of one signal due to all signals present:

$$C_i \doteq \left[\left(\frac{V_i}{2}\right)^2 - |\Psi_{(\bar{a}_i)}|^2\right] \Big/ \left(\frac{V_i}{2}\right)^2. \tag{38}$$

The approximate $N$ signal result is (Table III):

$$C_1 \approx \left[\left(\frac{V_1}{2}\right)^2 + 2\sum_{l=2}^{N}\left(\frac{V_l}{2}\right)^2\right], \quad \text{(Raman-Nath)} \tag{39a}$$

$$C_1 \approx \frac{1}{3}\left[\left(\frac{V_1}{2}\right)^2 + 2\sum_{l=2}^{N}\left(\frac{V_l}{2}\right)^2\right], \quad \text{(Bragg)}. \tag{39b}$$

The compression effect is three times smaller in the Bragg regime. Note that the contribution due to other signals is double the contribution due to self-compression. This is associated with diffraction into second-order intermodulation modes in the zeroth diffraction order. The process of compression of one signal due to another signal is called cross modulation.

*Cross Modulation $M_{i,j}$*

Cross modulation is defined as the fractional change in the diffraction efficiency of a signal ($V_i$) due to the presence of a finite second signal ($V_j$):

$$M_{i,j} \doteq \frac{|\Psi_{(\bar{a}_i)}(V_i, 0)|^2 - |\Psi_{(\bar{a}_i)}(V_i, V_j)|^2}{|\Psi_{(\bar{a}_i)}(V_i, 0)|^2}. \tag{40}$$

For small signals, (Tables II and III) the cross modulation due to a signal is twice its diffraction efficiency in the Raman-Nath regime, but only two-thirds its diffraction efficiency in the Bragg regime.

Fig. 5 shows the theoretical cross modulation on a small *CW* signal $|V_1/2|^2 = 0.01$ due to signal $V_2$ as a function of the intensity of the second signal $|V_2/2|^2$. Corresponding experimental data for the Bragg regime were measured by applying 100 percent square wave amplitude modulation (500 Hz) to signal $V_2$, while measuring the percent intensity modulation on mode $\Psi^1_{(1,0)}$.

*Intermodulation*

Intermodulation is the generation of responses corresponding to combination tones of input signals. The highest intensity intermodulation modes are the second-order modes $\Psi^0_{(\bar{a}_i - \bar{a}_j)}$, which correspond to difference frequencies, e.g., $f_i - f_j$. The intensities are equal to the products of the corresponding principal diffraction efficiencies in the Raman-Nath regime, but are four times lower in the Bragg regime. The difference modes are in the zeroth diffraction order ($G = 0$), which will not overlap the first-order provided input frequencies are restricted to an octave band. Then difference modes do not spatially interfere with the principal diffraction modes. However, diffraction to these modes is an important source of

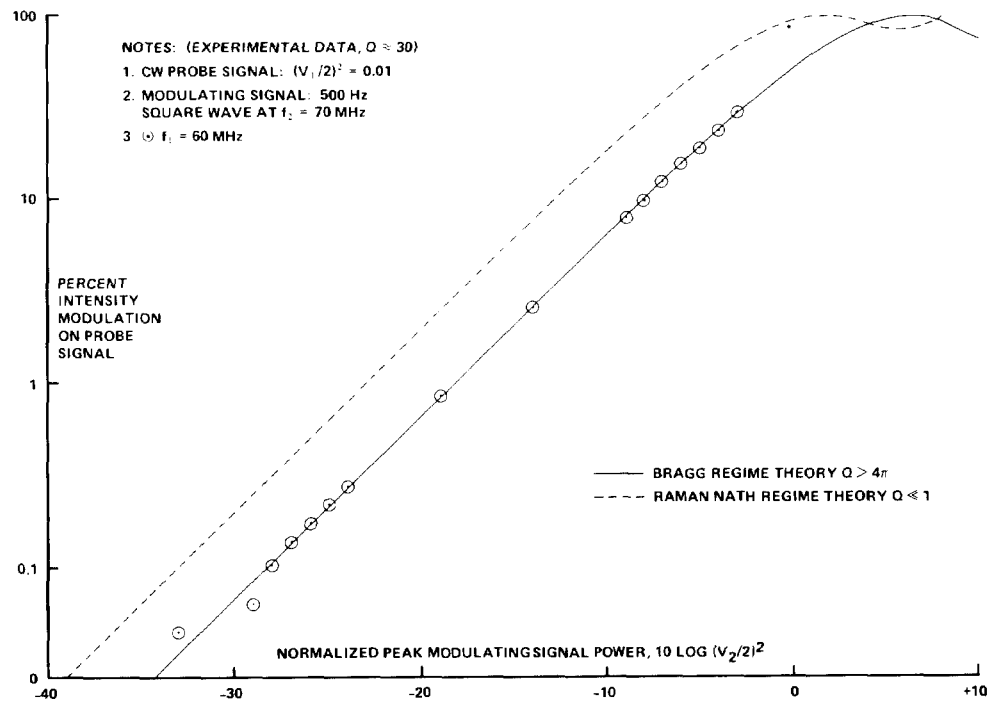


Fig. 5. Cross modulation.

compression distortion, cross modulation, and limited peak diffraction efficiency in the principal first-order modes.

*Sum Frequency*

Modes $\Psi^2_{(\bar{a}_i-\bar{a}_j)}$, corresponding to the sum frequency $f_i + f_j$, occur in the second diffraction order ($G = 2$). They are equal in intensity to the corresponding difference modes for Raman-Nath diffraction. However, they are suppressed in Bragg diffraction; numerical analysis of the coupled mode equations (12) is required to evaluate the amplitudes in each particular case. The sum modes also do not overlap the Principal modes provided input frequencies are restricted to an octave band.

*Third-Order Intermodulation*

Modes $\Psi^1_{(2\bar{a}_i-\bar{a}_j)}$ corresponding to frequencies $2f_i - f_j$ are third-order modes falling in the first diffraction order ($G = 1$). They interfere with the principal modes as spurious sideband responses. In conventional radio frequency analysis nomenclature, these responses are "two-tone third-order intermodulation products." Third-order intermodulation level is of great importance in large dynamic range multifrequency applications such as spectrum analysis and optical information processing [1], [3], [7], [21].

The Bessel function intermodulation response in the Raman-Nath acoustooptic regime is well known [7]. The multifrequency coupled mode solutions show that third-order intermodulation intensity is suppressed by a factor of 9 in the Bragg regime (see Table III). The results of a two-tone ($V_1 = V_2 = V$) intermodulation experiment on a Bragg device are shown in Fig. 6 along with the Bragg and Raman-Nath theoretical curves for principal modes and third-order intermodulation modes. The principal modes (first-order) have a slope of 1 on the logarithmic plot. The intermodulation modes (third-order) have a slope of 3. The spurious free dynamic range is about 50 dB with diffraction efficiencies of $10^{-7}$ to $10^{-2}$. The background level at $10^{-7}$ is due to aperture diffraction sidelobes of the source beam truncated by the finite device aperture.

Realization of the maximum spurious free dynamic range requires drive electronics of excellent linearity so that intermodulation signals at the input to the acoustooptic device do not yield diffraction efficiency in excess of the intermodulation levels generated acoustooptically. A convenient single parameter linearity specification is the intercept-point, which is the extrapolated intersection of the linear portions of the first and third order two-tone responses as shown in Fig. 6. This concept is applicable to acoustooptic cells as well as electronic amplifiers [20]. For maximum linearity, the intercept of the drive amplifier should exceed the input power equivalent to the acoustooptic intercept point. This ranges from $(V/2)^2 = 2$ in the Raman-Nath regime to $(V/2)^2 = 6$ in the Bragg regime. A Bragg cell with 0.1 percent diffraction efficiency at 1 milliwatt drive level has a third-order intercept corresponding to two signals of 6 watts each or +44 dBm peak envelope power.

*Intermodulation Spectra*

The theoretical Bragg regime two-tone intermodulation spectrum for two equal signals of intensity $(V/2)^2 = 0.1$ is shown in Fig. 7. This illustrates the maximum spurious response if diffraction efficiencies are restricted to below 10 percent. Bragg regime experimental results are shown as well as the

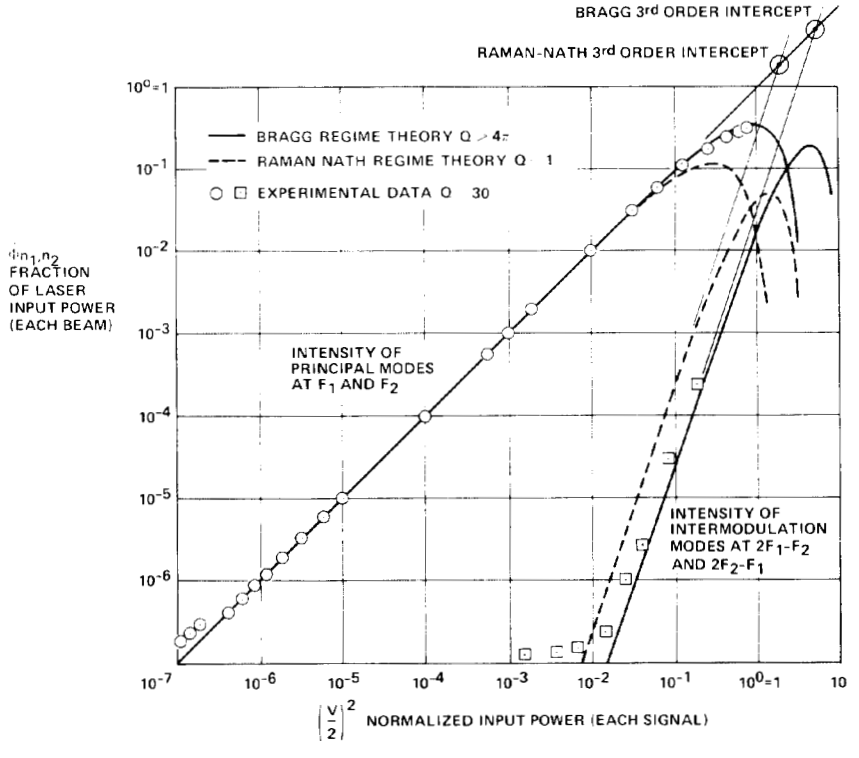


Fig. 6. Two-tone third-order intermodulation.

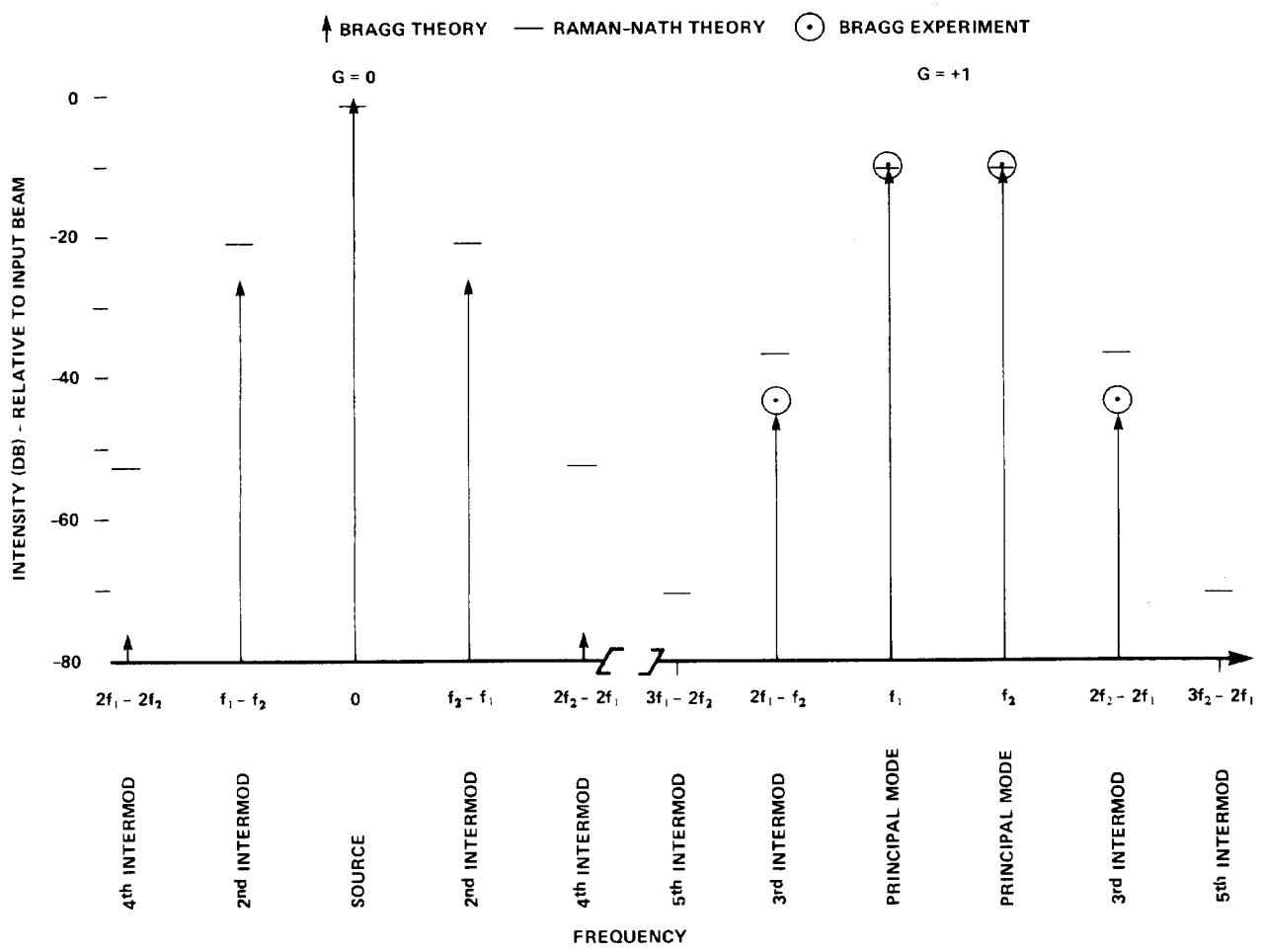


Fig. 7. Two-tone intermodulation spectrum, Bragg regime, $(V/2)^2 = 0.1$.

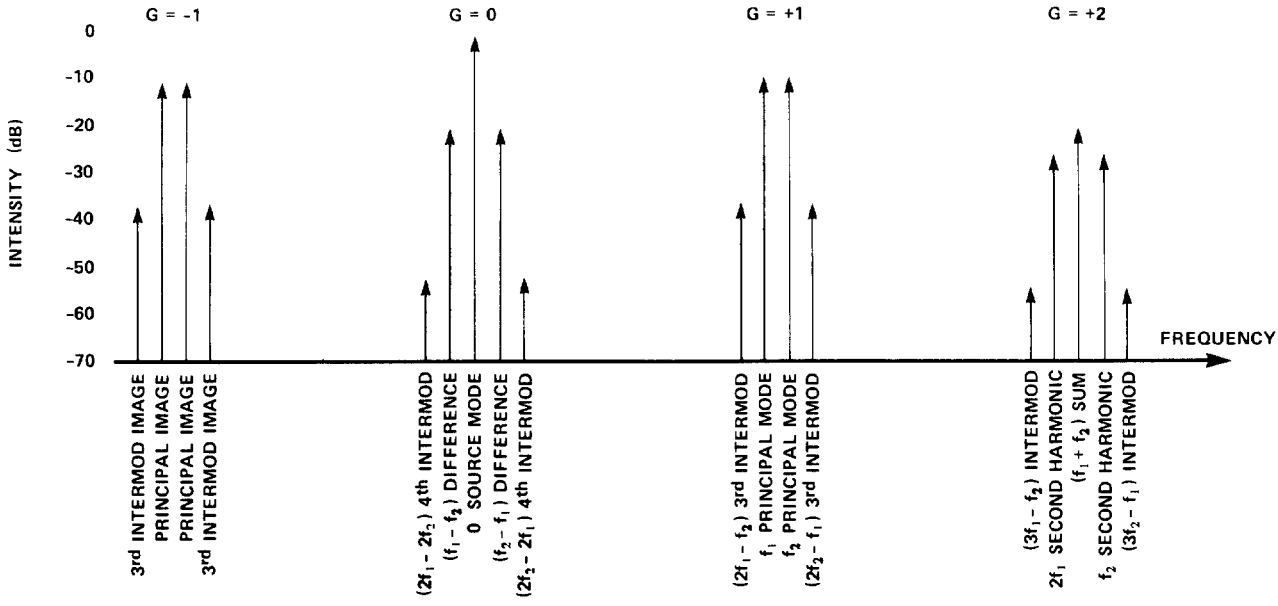


Fig. 8. Two-tone intermodulation spectrum, Raman–Nath regime, $(V/2)^2 = 0.1$.

corresponding theoretical levels in the Raman-Nath limit. All spurious responses with intensities within 80 dB of the source mode are shown for the 0 and +1 orders.

The Raman-Nath regime two-tone intermodulation spectrum is shown in Fig. 8. All modes within 70 dB of the source mode are shown for orders $G = -1, 0, +1, +2$. Appropriate nomenclature is noted. The signal levels are $(V/2)^2 = 0.1$.

*Intermodulation: Three-Tone Third-Order*

A less common standard for intermodulation response is the three-tone third-order intermodulation level. This is applicable in the presence of three or more signals which result in modes of the type $\Psi_{(\pm\bar{a}_i \pm \bar{a}_j \pm \bar{a}_k)}$ including first diffraction order modes $\Psi^1_{(\bar{a}_i + \bar{a}_j - \bar{a}_k)}$. If the three strongest simultaneous signals have comparable amplitudes, such intermodulation modes can be the most intense spurious responses in the first diffraction order. For equal amplitude signals the intensity is four times greater (see Table III) than the two-tone third-order modes. The nine-fold intermodulation suppression in the Bragg regime applies to these modes.

## IV. Conclusions

The derived coupled mode equations for multifrequency acoustooptic diffraction are useful for the quantitative and qualitative analysis of various effects which limit the diffraction efficiency and dynamic range in multifrequency applications. These include compression of the diffraction efficiency, cross modulation between beams, depletion of the source beam, and generation of various spurious intermodulation beams, particularly the third-order intermodulation.

Analytic solutions for the diffraction modes are found for $N$ independent signals in the Raman-Nath regime limit (thin ultrasonic gratings) and two independent signals in the Bragg regime limit (thick ultrasonic gratings). Bragg results for small amplitudes can be generalized to $N$ signals. Various results, including small signal approximation results, are summarized in Tables I-IV. The Raman-Nath results are generalized from well-known Bessel function solutions. The Bragg regime results indicate that all nonlinear responses considered are suppressed by a factor of at least two by the use of thick gratings. This is related to the suppression of interaction pathways outside the 0 and +1 orders. Source beam depletion is reduced by a factor of two, compression and cross modulation are reduced by a factor of three, and third-order intermodulation is reduced by a factor of nine. This is supported by experimental measurements of the various effects in good agreement with the Bragg limit theory.

## Appendix A

### Analytic Solution of the Bragg Regime Coupled Mode Equations for $N = 2$

If wavevector mismatch is neglected for modes in order $G = 0$ and $G = +1$, the Bragg regime coupled mode equations take the form:

$$\frac{d}{dz}\Psi^0_{(\bar{n})} = \sum_{m=1}^{N}\left(\frac{V_m}{2L}\right)\Psi^1_{(\bar{n}+\bar{a}_m)} \tag{A1a}$$

$$\frac{d}{dz}\Psi^1_{(\bar{n})} = -\sum_{m'=1}^{N}\left(\frac{V_{m'}}{2L}\right)\Psi^0_{(\bar{n}-\bar{a}_{m'})}. \tag{A1b}$$

The equation sets may be decoupled by differentiation and cross substitution, yielding,

$$\frac{d^2}{dz^2}\Psi^0_{(\bar{n})} + \sum_{m=1}^{N}\left(\frac{V_m}{2L}\right)\sum_{m'=1}^{N}\left(\frac{V_{m'}}{2L}\right)\Psi^0_{(\bar{n}+\bar{a}_m-\bar{a}_{m'})} = 0 \tag{A2a}$$

$$\frac{d^2}{dz^2}\Psi^1_{(\bar{n})} + \sum_{m=1}^{N}\left(\frac{V_m}{2L}\right)\sum_{m'=1}^{N}\left(\frac{V_{m'}}{2L}\right)\Psi^1_{(\bar{n}+\bar{a}_m-\bar{a}_{m'})} = 0. \tag{A2b}$$

Initial conditions for the second-order equations are obtained by combining the given conditions (14) with the first-order equation (A1).

*Initial Conditions:*

$$\Psi^0_{(\bar{n})} = 1, \quad (\bar{n}) = (\bar{0}) \tag{A3a}$$

$$\Psi^0_{(\bar{n})} = 0, \quad (\bar{n}) \neq (\bar{0}) \tag{A3b}$$

$$\Psi^1_{(\bar{n})} = 0 \tag{A3c}$$

$$\frac{d}{dz}\Psi^0_{(\bar{n})} = 0 \tag{A4a}$$

$$\frac{d}{dz}\Psi^1_{(\bar{n})} = -\frac{V_m}{2L}, \quad (D = 1) \tag{A4b}$$

$$\frac{d}{dz}\Psi^1_{(\bar{n})} = 0, \quad (D \neq 1). \tag{A4c}$$

For $N = 2$, (A2a) takes the form

$$4L^2\left(\frac{d^2\Psi^0_n}{dz^2}\right) + (V_1^2 + V_2^2)\Psi^0_n = -V_1V_2[\Psi^0_{n+1} + \Psi^0_{n-1}] \tag{A5}$$

where

$$\Psi^0_n \equiv \Psi^0_{(\bar{n})} \equiv \Psi^0_{(n,-n)}. \tag{A6}$$

Equation (A5) can be solved by assuming ascending power series solutions:

$$\Psi^0_n = \sum_{r=0}^{\infty} a_{nr}\, z^r. \tag{A7}$$

Substituting the power series solutions into the differential equation yields the recursion relation:

$$4L^2(r+2)(r+1)a_{n(r+2)} + [V_1^2 + V_2^2]\, a_{nr} = -V_1V_2[a_{(n-1)r} + a_{(n+1)r}]. \tag{A8}$$

The initial conditions (A3, 4) establish the first terms in the solution series:

$$a_{n0} = 1, \quad n = 0 \tag{A9a}$$

$$a_{n0} = 0, \quad |n| > 0 \tag{A9b}$$

$$a_{n1} = 0. \tag{A9c}$$

The remaining terms are found using the recursion relations. The general expression found for the coefficients is

$$a_{nr} = \sum_{s=0}^{[(M-|n|)/2]} C_{M,n,s} \frac{(-1)^M}{(r)!} \left(\frac{V_1 V_2}{4L^2}\right)^{2s+|n|} \cdot \left(\frac{V_1^2 + V_2^2}{4L^2}\right)^{M-|n|-2s} \tag{A10}$$

where $[x]$ denotes greatest integer not greater than $x$ [17], and

$$M \doteq \frac{r}{2} \tag{A11}$$

$$C_{M,n,s} = \frac{M!}{(M - |n| - 2s)\,!\,(s + |n|)\,!s!}. \tag{A12}$$

$C_{M,n,s}$ is a combinatorial expression [18], which gives the number of partitions of a set of size $M$ into subsets of sizes $(M - |n| - 2s)$, $(s + |n|)$ and $s$.

With series solutions obtained for the zero-order modes $\Psi^0_{n,-n}$, the first-order mode amplitudes $\Psi^1_{(n,-n+1)}$ can be obtained by direct integration of the first-order equations (A1b) subject to the initial conditions (A3). The results are

$$\Psi^1_{(n,-n+1)} = \sum_{r=0}^{\infty} \left(\frac{-1}{r+1}\right) \left[\frac{V_1}{2L} a_{(n-1)r} + \frac{V_2}{2L} a_{nr}\right] z^{r+1}. \tag{A13}$$

Mode amplitudes at the end of the interaction are obtained with $z = L$.

## Acknowledgments

We wish to thank Dr. C. B. Crumly for a number of discussions which encouraged our pursuit of these investigations on multifrequency acoustooptic diffraction; and Dr. I. C. Chang for many helpful discussions concerning coupled mode analysis of acoustooptics and for his independent verification of a number of the algebraic results. We also wish to thank T. Mannigel for his careful work in producing accurate computer plots of complicated series solutions, including the important observation of numerical similarity of pairs of solutions in the Bragg and Raman-Nath regimes. Drs. Chang and Crumly were very helpful in reading the manuscript.

## References

[1] B. Lambert, "Wideband Instantaneous Spectrum Analyzers Employing Delay Line Modulators," *IRE National Convention Record*, Vol. 10, part 6, pp. 69-78, March 1962.
[2] T. W. Cole, "An Electrooptical Radio Spectrograph," *Proc. IEEE*, Vol. 61, No. 9, September 1973, pp. 1321-1323.
[3] D. L. Hecht, "Broadband Acoustooptic Spectrum Analysis," *1973 IEEE Ultrasonics Symposium Proceeding*, IEEE Catalog Number 73 CHO 807-8SU, New York, 1973, pp. 98-100.
[4] M. King, W. R. Bennet, L. B. Lambert, and M. Arm, "Real Time Electrooptical Signal Processing with Coherent Detection," *Applied Optics*, Vol. 6, No. 8, August 1967, pp. 1367-1375.
[5] A. Korpel, S. N. Lotsoff, and R. L. Whitman, "The Interchange of Time and Frequency in Television Displays," *Proc. IEEE*, Vol. 57, No. 2, Feb. 1969.
[6] R. W. Damon, W. T. Maloney, and D. H. McMahon, "Interaction of Light with Ultrasound: Phenomena and Applications" in *Physical Acoustics Principals and Methods*, Vol. VII, W. P. Mason and R. N. Thurston, Academic Press, 1970, pp. 273-367.
[7] K. Preston, Jr., *Coherent Optical Computers*, McGraw Hill 1972, p. 166.
[8] A. Vander Lugt, "Coherent Optical Processing," *Proc. IEEE*, Vol. 62, No. 10, October 1974, pp. 1300-1319.
[9] D. L. Hecht, T. Mannigel, J. Rieden, and M. Silver, "Wideband Multifrequency Recording Using Acoustooptics," *1973 Electrooptic Systems Design Conference Proceedings*, pp. 112-116.
[10] G. Hrbek and W. Watson, "A High Speed Laser Alphanumeric Generator," *Proceedings of the Electrooptical Systems Design Conference 1971 East*, pp. 271-275.
[11] D. L. Hecht, "Acoustooptic Nonlinearities in Multifrequency Acoustooptic Diffraction," VIII International Quantum Electronics Conference, San Francisco, June 1974, Paper X10.
[12] W. R. Klein and B. D. Cook, "Unified Approach to Ultrasonic Light Diffraction," *IEEE Trans. on Sonics and Ultrasonics*, July 1967, p. 123.
[13] W. R. Klein, B. D. Cook, and W. G. Mayer, "Light Diffraction by Ultrasonic Gratings," *Acustica*, Vol. 15, pp. 67-74, January 1965.
[14] R. W. Dixon, "Acoustic Nonlinear Frequency Mixing Detected Using Optical Bragg Diffraction," *Applied Physics Letters*, Vol. 11, No. 11, pp. 340-344, 1 December 1967.
[15] R. W. Dixon, "Acoustic Diffraction of Light in Anisotropic Media," *IEEE J. Quantum Electronics*, Vol. QE-3, No. 2, February 1967.
[16] R. Extermann and G. Wannier, Helv. Phys. Acta, 9 (1936), 520; M. Born and E. Wolf, *Principles of Optics*, 3rd Edition, Pergamon Press 1965, p. 598.
[17] C. B. Allendoerfer and C. O. Oakley, *Principles of Mathematics*, McGraw Hill, 1955, p. 131.
[18] M. Parzen, *Modern Probability Theory and Its Applications*, John Wiley, 1960, pp. 39-40.
[19] M. Abramovitz and I. A. Stegun (Editors), *Handbook of Mathematical Functions*, National Bureau of Standards (1964), p. 360.
[20] F. C. McVay, *Electronic Design*, Vol. 3, Feb. 1, 1967, p. 70.
[21] M. King, "Measurement and Application of Dynamic Range for Holographic Storage Media," *Applied Optics*, Vol. 11, No. 4, p.791 (1972).